www.nature.com/aps

Acta Pharmacologica Sinica

ARTICLE

Calcipotriol abrogates cancer-associated fibroblast-derived IL-8-mediated oxaliplatin resistance in gastric cancer cells via blocking PI3K/Akt signaling

Zhen-xiong Zhao[1,2], Yan-qiu Zhang[2,3], Hui Sun[2,4,5], Zi-qi Chen[6], Jin-jia Chang[2,3], Xin Wang[2,4,5], Xu Wang[2,4,5], Cong Tan[2,4,5], Shu-juan Ni[2,4,5], Wei-wei Weng[2,4,5], Meng Zhang[2,4,5], Lei Wang[2,4,5], Dan Huang[2,4,5], Yun Feng[7], Wei-qi Sheng[2,4,5] and Mi-die Xu[2,4,5]

Activation of vitamin D receptor (VDR) in cancer-associated fibroblasts (CAFs) has been implicated in hesitating tumor progression and chemoresistance of several human malignancies. Yet, the role of VDR in CAF-induced chemotherapy resistance of gastric cancer (GC) cells remains elusive. In this study we first conducted immunohistochemistry analysis on tissue microarrays including 88 pairs of GC and normal mucosa samples, and provided clinical evidence that VDR was mainly expressed in gastric mucous cells but almost invisible in CAFs, and VDR expression was negatively correlated with malignant clinical phenotype and advanced stages, low VDR expression confers to poor overall survival rate of patients with GC. In a co-culture system of primary CAFs and cancer cells, we showed that treatment of HGC-27 and AGS GC cells with VDR ligand calcipotriol (Cal, 500 nM) significantly inhibited CAF-induced oxaliplatin resistance. By using RNA-sequencing and Human Cytokine Antibody Array, we demonstrated that IL-8 secretion from CAFs induced oxaliplatin resistance via activating the PI3K/AKT pathway in GC, whereas Cal treatment greatly attenuated the tumor-supportive effect of CAF-derived IL-8 on GC cells. Taken together, this study verifies the specific localization of VDR in GC tissues and demonstrates that activation of VDR abrogates CAF-derived IL-8-mediated oxaliplatin resistance in GC via blocking PI3K/Akt signaling, suggesting vitamin D supplementation as a potential strategy of enhancing the anti-tumor effect of chemotherapy in GC.

Keywords: gastric cancer; cancer-associated fibroblasts; Vitamin D receptor; calcipotriol; PI3K/AKT pathway; IL-8; oxaliplatin; chemoresistance; tumor microenvironment

Acta Pharmacologica Sinica (2023) 44:178–188; https://doi.org/10.1038/s41401-022-00927-1

INTRODUCTION

Gastric cancer (GC) ranks as the fifth most common cancers and the fourth fatal cause of cancer death worldwide, with more than one million new cases and about 769,000 deaths globally in 2020 [1]. Despite the improvement in the treatment for GC, patients with surgically unresectable tumors have only around one-year overall survival under combination chemotherapy [2]. As the proportion of patients with advanced GC at the initial diagnosis is as high as 50%–80%, these patients have lost the opportunity for radical resection at the first diagnosis. Systemic therapy (including perioperative chemotherapy and postoperative adjuvant chemotherapy) can relieve symptoms, and improve survival and quality of life, thus is recommended by the NCCN guideline for the management of patients with locally advanced or metastatic GC [3]. At present, oxaliplatin combined with 5-fluorouracil has been widely used as the first-line chemotherapy in the treatment of GC [3]. However, the widespread presence of chemoresistance limits the effectiveness and the clinical application of oxaliplatin and results in treatment failure in the majority of cases [4]. Inherent or acquired resistance mechanisms of patients are the main obstacles to the GC chemotherapy, and the molecular mechanisms remain to be elucidated.

More and more evidence testified that the cancer microenvironment plays a critical role in the chemoresistance and progression of many cancers [5, 6]. The tumor microenvironment (TME) consists of complex components such as cancer-associated fibroblasts (CAFs), immune cells, endothelial cells as well as cytokines, chemokines and extracellular matrix. CAFs are key functional regulators in tumors. Through releasing regulatory factors, synthesizing and reshaping extracellular matrix, or regulating the biological characteristics of tumor cells through cell-to-cell contact, CAFs affect the occurrence and development of tumors, as well as chemotherapy resistance [7, 8]. CAFs are the major stromal part of GC and contribute to malignancy such as

[1]Department of Gastric Surgery, Fudan University Shanghai Cancer Center, Shanghai 200032, China; [2]Department of Oncology, Shanghai Medical College, Fudan University, Shanghai 200032, China; [3]Department of Gastrointestinal Medical Oncology, Fudan University Shanghai Cancer Center, Shanghai 200032, China; [4]Department of Pathology, Fudan University Shanghai Cancer Center, Shanghai 200032, China; [5]Institute of Pathology, Fudan University, Shanghai 200032, China; [6]Shanghai Municipal Hospital of Traditional Chinese Medicine, Shanghai University of Traditional Chinese Medicine, Shanghai 200080, China and [7]Department of Gastroenterology, Shanghai General Hospital, School of Medicine, Shanghai Jiao Tong University, Shanghai 200080, China
Correspondence: Yun Feng (yun.feng2@shgh.cn) or Wei-qi Sheng (shengwq@shca.org.cn) or Mi-die Xu (midiexu12@fudan.edu.cn)
These authors contributed equally: Zhen-xiong Zhao, Yan-qiu Zhang, Hui Sun, Zi-qi Chen

Revised: 25 May 2022 Accepted: 25 May 2022
Published online: 8 June 2022

proliferation and migration of cancer cells [9]. It has been reported that CAFs derived IL-8 induced chemoresistance in human GC cells via activation of NF-κB signaling and up-regulation of ATP-binding cassette subfamily B member 1 (ABCB1) [10]. Moreover, IL-8 secreted from CAFs could activate normal ovarian fibroblasts, stimulate cell proliferation, increase the IC_{50} of cisplatin and promote stemness in human ovarian cancer via activating Notch3-mediated signaling [11]; and could promote gallbladder cancer cell proliferation by up-regulating Neuropilin-1 (NRP1) [12]. However, by activating intracellular tumor suppressor signaling pathways in tumor cells, the malignant progression induced by CAFs can be counteracted. Therefore, it is quite necessary to consider cancer cells and the surrounding microenvironment as a whole to study drug resistance.

Vitamin D is a prohormone that is attached to the Vitamin D Receptor (VDR) which exerts a wide range of functions in vivo. Several preclinical studies showed that Vitamin D supplementation significantly reduced the risk of metastasis and fatality in some patients with digestive tract cancer [13–15]. In pancreatic cancer, Vitamin D analog calcipotriol (Cal) abrogated stromal mediated tumoral supportive effect by targeting cancer-associated pancreatic stellate cells [16]. Moreover, activation of VDR shows protective effects by hesitating the oncogenic role of stromal fibroblasts in colorectal cancer [17]. In GC, the expression of VDR in normal, premalignant, and malignant gastric tissues showed a decline linear trend, and the expression of VDR in GC tissues was significantly lower than that in normal tissues [18]. However, VDR expression has no correlation with proliferation marker Ki67, or apoptosis marker CK18 in GC tissues [19]. In the present study, we aimed to confirm the expression and clinicopathological correlation of VDR expression in GC tissues and investigate the cell type in which VDR is located, as well as the role of VDR in CAF-mediated chemoresistance. The results would further uncover the therapeutic actions of VDR on GC as well as the related mechanism and would provide a potential strategy for the clinical application of VDR on GC therapy.

MATERIALS AND METHODS

Patients

The KmPlot online database (https://kmplot.com/analysis/), which includes gene expression profile and prognostic information of 875 GC samples were used for analyzing overall survival (OS). A series of previously applied tissue microarrays (TMA) [20, 21] from the tissue bank of Fudan University Shanghai Cancer Center (FUSCC), which enrolled GC 88 patients who underwent tumor resection during 2007–2009, were used for immunochemistry (IHC) analysis of VDR expression. The follow-up of patients was performed every three months during the first postoperative year and one year thereafter until May 30, 2021. This study was approved by The Research Ethics Committee of FUSCC, and all patients had signed informed consent.

Cell culture and isolation of CAFs

Human GC cell lines, HGC-27 and AGS were cultured as previously reported [20, 21]. Cancer-associated fibroblasts (CAFs) and normal fibroblasts (NFs) were isolated from human GC and normal tissues of patients who underwent surgery in the Department of Gastric Surgery, FUSCC. Tissues were firstly cleaned in phosphate buffer saline (PBS, Cat# abs962, Absin, Shanghai, China) added with 100 U/mL penicillin and 100 μg/mL streptomycin (Cat# 15140122, Gibco, Gaithersburg, MD, USA) and then cut into small pieces. Type IV collagenase (0.1%, Cat# C5138, Sigma-Aldrich, Darmstadt, Germany) was applied to digest tissues at 37 °C and 5% CO_2 for two hours. Then fetal bovine serum was added to stop digestion. After centrifugation (800 × *g*, 5 min), cells were transferred in a new culture dish. CAFs and NFs were purified after two generations and then used for functional experiments.

Preparation of conditioned medium (CM)

Fibroblasts were seeded in RPMI-1640 medium (Cat# C22400500BT, Gibco, Gaithersburg, MD, USA) with 10% fetal bovine serum (Cat# 10270-106, Gibco, Gaithersburg, MD, USA) for several days and the culture medium was discarded at cell densities of 70%–90% confluence. Then fresh serum-free RPMI-1640 medium was added into the dish to culture fibroblasts for 48 h. The supernatant was collected, centrifugated at 1000 × *g* for 5 min, and labeled as CAF-CM.

CAF-cancer cell co-culture system

HGC-27 or AGS cells (1×10^5) were seeded on the bottom of the six-well plate (Cat# 3516, Corning, NY, USA) and CAFs (5×10^4) were incubated in the tissue culture plate insert (Cat# 14111, Labselect, Hefei, China), which is the upper chamber of a 6-well Transwell apparatus. The insert contained a membrane of 0.4 μm pore size which allowed the exchange of supernatants but not cells. After one week of co-culture, cells were collected for further experiments.

Immunofluorescence for cells

CAFs and NFs were fixed on coverslips with 4% paraformaldehyde for 30 min and treated with 0.1% Triton X-100 for half an hour. After incubated in 5% bovine serum albumin (BSA, Cat# G5001, Servicebio, Wuhan, China) for 60 min, primary antibodies against Fibroblast Activation Protein (FAP) (dilution 1:100, Cat# 66562, CST, Boston, MA, USA), anti-alpha-smooth muscle actin (α-SMA) (dilution 1:100, Cat# BM0002, Boster, Wuhan, China) and Vimentin (dilution 1:100, Cat# 5741, CST, Boston, MA, USA) were applied to incubate with cells at 4 °C overnight, respectively. Secondary antibodies included FITC Conjugated AffiniPure Goat Anti-mouse IgG (dilution 1:100, Cat# BA1101, Boster, Wuhan, China), Cy3 conjugated Goat Anti-Rabbit IgG (dilution 1:100, Cat# GB21303, Servicebio, Wuhan, China) and FITC conjugated Goat Anti-Rabbit IgG (dilution 1:100, Cat# GB22303, Servicebio, Wuhan, China). After incubation for 1 h at 37 °C, the antibody was removed. Then, nuclei cells were incubated with DAPI (Cat# G1012, Servicebio, Wuhan, China) for 30 min. Last, an antifade agent was used before the examination.

Double immunofluorescence staining for tissues

After deparaffinization and rehydration, antigen retrieval was performed in paraffin-embedded samples. Then, objective tissues were covered with 3% BSA at room temperature for 30 min. After blocking, the blocking solution was thrown away. Slides were incubated with the first primary antibody goat-anti-human FAP (dilution 1:200, Cat# ab207178, Abcam, Cambridge, UK) at 4 °C overnight, and placed in a wet box, which containing a little water. After CY3-TSA solution and microwave treatment, primary antibodies and secondary antibodies combined with tissue were removed, slides were then incubated with second primary antibody IL-8 (1:400, Cat# 27095-1-AP, Proteintech, Wuhan, China) at 4 °C overnight, and second corresponding secondary antibody marked with HRP, followed by FITC-TSA solution and microwave treatment. Then slides were incubated with DAPI solution at room temperature for 10 min, kept in dark place. Eventually, images were detected and collected by a slice scanner.

siRNA transfection

Cancer cells of 60% confluent were seeded in six-well plates for transfection. A total of 5 μL Lipofectamine® RNAiMAX Reagent (Cat# 13778150, Invitrogen, Carlsbad, CA, USA) and 5 μL siRNA (RIBOBIO, Guangzhou, China) were separately incubated in 100 μL Opti-MEM Medium (Cat# 31985070, Gibco Gaithersburg, MD, USA), and then mixed and incubated together for 15 min. Finally, the mixture was added to cell plates for 48 h, and cells were harvested for further tests. The sequence for siRNA targeting VDR and CXCR2 was listed as follows: VDR siRNA1, 5′-AGCGCATCATTGCCATACT-3′,

VDR siRNA2, 5′-GTCAGTTACAGCATCCAAA-3′; CXCR2 siRNA1, 5′-GAAGCGCTACTTGGTCAAA-3′, CXCR2 siRNA2, 5′-CGAAGGACCGTC-TACTCAT-3′.

Reagents and antibodies

Two PI3K/AKT pathway inhibitors, 3-methyladenine (5 mM, Cat# HY-19312) and perifosine (10 μM, Cat# HY-50909) were purchased from MedChemExpress (MCE, New Jersey, USA). Western blot antibodies for P-PI3K (Cat# 4228, CST), PI3K (Cat# 4257, CST), P-AKT (Cat# 4060, CST), AKT (Cat# 4685, CST) were purchased from Cell Signaling Technology (CST, Boston, MA, USA), 1:1,000 dilution. Other antibodies include VDR (Cat# sc-13133, Santa Cruz, Dallas, TX, USA), CXCR2 (Cat# sc-7304, Santa Cruz, Dallas, TX, USA), PARP-1 (Cat# sc-8007, Santa Cruz, Dallas, TX, USA), cleaved PARP-1 (Cat# sc-56196, Santa Cruz, Dallas, TX, USA), caspase 3 (Cat# T40044, Abmart, Shanghai, China), monoclonal mouse anti-β-actin (1:5000 dilution, Cat# AF7018, Affinity, Liyang, China), secondary antibody-goat anti-Rabbit & Mouse (Cat# M21003, Abmart, Shanghai, China).

Cell viability assay

HGC-27 and AGS cells exposed to oxaliplatin(Cat# S1224, Selleck, Houston, TX, USA) were assessed by Cell Counting Kit (CCK-8; Cat# 40203ES60, Yeasen, Shanghai, China). A total of 1000 cells were seeded in 96-well plates (Cat# 3599, Corning, NY, USA) for 24 h and then treated with different doses of oxaliplatin (0 μM, 5 μM, 10 μM, 20 μM, 40 μM, 80 μM) for 24 h. Following the manufacturer's instructions, the culture medium was discarded and CCK-8 was added into a fresh medium to incubate cells at 37 °C for 2 h in darkness. The absorbance at 450 nm was measured by a microplate reader (#SpectraMaxABC, Molecular Devices, Shanghai, China).

Apoptosis assay

HGC-27 and AGS cells were treated with oxaliplatin or Cal (500 nM, Cat# HY-10001, MCE, New Jersey, USA) in the presence or absence of CAFs and then digested by 0.25% trypsin. After centrifugation, Annexin V-FITC/PI Apoptosis Detection Kit (Cat# 40302ES60, Yeasen, Shanghai, China) was used to detect apoptosis. After incubation with 5 μL Annexin V-FITC and 10 μL PI Staining Solution for 15 min, cells were subjected to flow cytometry analysis immediately by flow cytometer (#CytoFlex, Beckman, Brea, CA, USA). Annexin V^+/PI^- means early apoptosis while Annexin V^+/PI^+ indicates late apoptosis.

RNA sequencing

Total RNA of cells was extracted using TRNzol (Cat# DP424, Tiangen, Beijing, China). The quality control, library preparation, and RNA sequencing analysis, and KEGG enrichment analysis were carried out by GENEWIZ (Suzhou, China). There are three replicates for control and experimental groups. Adjusted P value ≤ 0.05 was set to detect differentially expressed genes.

Human cytokine antibody array

The culture media of CAFs and HGC-27 cells was detected by RayBiotech Human Cytokine Antibody Arrays V kit (Cat# AAH-CYT-5, Atlanta, GA, USA) which could detect eighty different kinds of cytokines. Following the manufacturer's instructions, after being blocked, the array was incubated with 1 mL conditioned medium at 4 °C overnight. Next, the membrane was incubated with 1 mL of the prepared Biotinylated Antibody Cocktail and washed twice. After incubation with HRP-Streptavidin and preparation for chemiluminescence detection, the membrane was transferred to the imaging system (#Tanon 5200 Multi, Tanon, Shanghai, China) and exposed. Gray values were calculated after normalization (with background subtraction).

Enzyme-linked immunosorbent assay (ELISA)

CAFs and HGC-27 cells were cultured in RPMI-1640 with 10% fetal bovine serum for several days until cell densities reached 90% confluence. Then fresh serum-free RPMI-1640 medium was added. After 24 h the supernatant was collected for ELISA assay. IL-8 was detected by ELISA kit (Cat# AB-J0472B, Abmart, Shanghai, China) following the manufacturer's instruction.

Immunohistochemistry

After being deparaffinized and rehydrated, antigen retrieval was performed on the paraffin section of gastric normal and tumor tissues. Samples were incubated with antibodies specific for VDR (Cat# sc-13133, Santa Cruz, Dallas, TX, USA) at 4 °C overnight. The next day, immunodetection was performed according to the manufacturer's instruction. IHC images of VDR were analyzed at ×20 magnification using HALO (Version 2.3) software package and were calculated based on the cell localized biomarker signal. Immunostaining of VDR protein was assessed by determining the H-score, a semi-quantitative approach combining both immunostaining intensity and percentages of positive cells of the tumor as previously reported [22].

In vivo experiments

All animal experiments were approved by the ethics committee of Experimental Animal Center, Fudan University Shanghai Cancer Center, Shanghai, China. A total of 1×10^7 HGC-27 cells were suspended in PBS and then inoculated into the five-week-old BALB/c-nude mice subcutaneously with or without 2×10^6 CAFs (5:1). Animals were then treated with PBS, or oxaliplatin (10 mg/kg, intraperitoneal) and/or Cal (60 mg/kg intraperitoneal) three times a week. Tumors were monitored every three days since the first treatment and tumor length (L) and width (W) were recorded. Tumor volume was calculated as L×W×W/2.

Statistical analysis

GraphPad Prism 9.0 statistical software was applied to carry out all statistical analyses. Data were shown as the means ± standard error of the mean (SEM). Paired t test, Mann-Whitney test, two-tailed χ^2 test, and unpaired Student's t-test were used in two-group comparisons, as appropriate. One-way ANOVA was used in multiple comparison tests. In all cases, a P value lower than 0.05 was considered statistically significant.

RESULTS

VDR expression in gastric mucous cells is associated with clinical features and outcomes of GC patients

To analyze VDR expression, we performed immunohistochemistry on tissue microarrays (TMA), including 88 pairs of GC and normal mucosa samples. We found that VDR mainly located in the cytoplasm and perinuclear regions of the gastric mucous cell. However, we found no positive immunostaining of VDR in the stroma of GC tissues (Fig. 1a). This indicated that the role of the VDR signal in GC may not be the same as that of pancreatic cancer and colorectal cancer [16, 17], and is not attributed to its activity in CAFs.

Analyzing the expression of VDR in GC cells, we found that there was no significant difference in VDR protein expression between GC and adjacent normal gastric mucosa ($P = 0.730$; Fig. 1a, b). VDR immunostaining H-score was statistically significant lower in GC samples from patients with poorer differentiation ($P = 0.012$; Fig. 1c), adenocarcinoma (AD) with mucus or signet ring cell (SRC, $P = 0.004$; Fig. 1d), deeper infiltration ($P = 0.004$; Fig. 1e), present of nervous invasion ($P = 0.008$; Fig. 1f), present of vascular invasion ($P = 0.040$; Fig. 1g), present of lymphatic metastasis ($P < 0.001$; Fig. 1h) and advanced clinical stage (TNM stage III + IV, $P < 0.001$; Fig. 1i). By using the cut-off value setting by the Youden's index (59.913718) of VDR immunostaining H-Score, we divided GC patients as low ($n = 59$) and high ($n = 29$) expression groups, and further analyzed the relationship between VDR expression level and clinicopathological features (Table 1). In

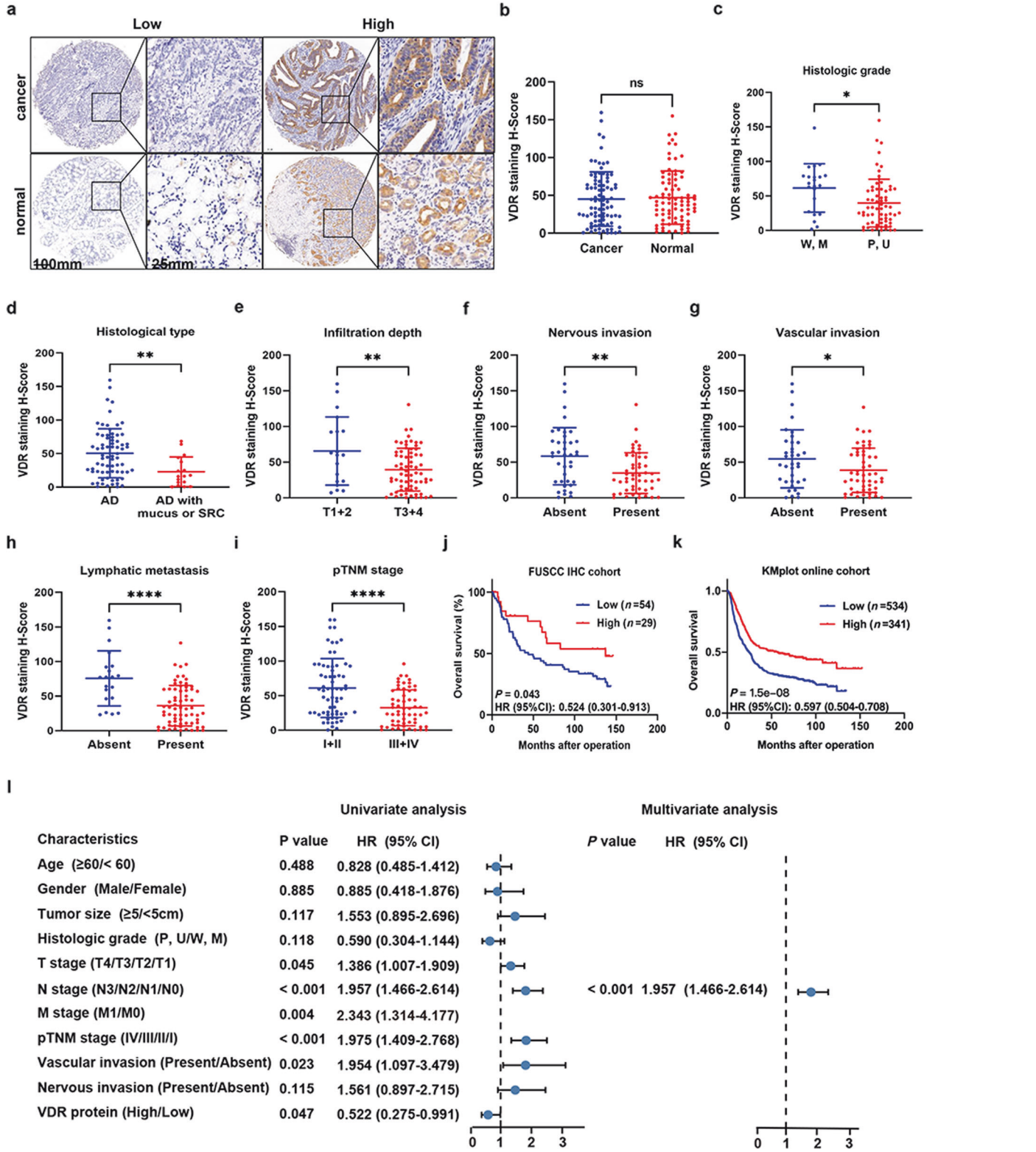

Fig. 1 Clinical relevance of VDR protein expression. a Representative immunohistochemical images of VDR protein expression in gastric tumors and normal gastric mucus (scale bar = 500/100 μm); **b** The semi-quantitative analysis of VDR protein expression between gastric tumors and normal gastric mucus; **c–i** The expression of VDR protein in indicated groups (*$P < 0.05$, **$P < 0.01$, ****$P < 0.0001$); **j** Kaplan–Meier survival curves with log-rank method depicting overall survival (OS) of GC patients ($n = 88$) based on VDR expression levels in GC tissues in the FUSCC cohort; **k** Kaplan–Meier survival curves with log-rank method depicting OS of GC patients ($n = 875$) based on VDR expression levels in GC tissues; **l** The univariate and multivariate Cox regression analysis for overall survival were performed in prespecified subgroups. W well; M moderate; P poor; U undifferentiated

Table 1. Clinical characteristics of GC patients

Variables		VDR expression		*P* value
		Low ($n = 59$)	High ($n = 29$)	
Age (year)	<60	33	13	0.327
	≥60	26	16	
Gender	Male	49	25	0.704
	Female	10	4	
Tumor size	<5 cm	42	17	0.238
	≥5 cm	17	12	
Histologic grade	Poor or undifferentiated	52	14	<0.001[a]
	Good or moderate	7	15	
pT stage	T1	1	4	0.024
	T2	9	5	
	T3	5	6	
	T4	44	14	
pN stage	N0	7	13	0.007[a]
	N1	8	3	
	N2	19	5	
	N3	25	8	
pM stage	M0	42	24	0.239
	M1	17	5	
pTNM stage	I	0	7	<0.001[a]
	II	12	9	
	III	31	8	
	IV	16	5	
Vascular invasion	Absent	22	14	0.324
	Present	37	15	
Nervous invasion	Absent	19	20	0.001[a]
	Present	40	9	

[a]All statistical tests were 2-sided. Significance level: $P < 0.05$.

addition, we found that VDR expression levels were tightly correlated with histologic grade ($P < 0.001$), pT stage ($P = 0.024$), pN stage ($P = 0.007$), pTNM stage ($P < 0.001$) and nervous invasion ($P = 0.001$). All these suggested that VDR expression was negatively correlated with malignant biological behaviors of GC cells.

Next, we explored the association of VDR level with the clinical outcome of patients with GC. As is shown in Fig. 1j, higher expression of VDR protein was correlated with significantly favorable OS (overall survival, $P = 0.043$). In addition, by using the KMplot online database (https://kmplot.com/analysis/), we confirmed that GC patients with high level of VDR mRNA had a favorable OS ($P = 1.5 \times 10^{-8}$) (Fig. 1k). However, multivariate Cox regression analysis of survival revealed that the relative level of VDR expression was not an independent protective factor of OS in patients with GC (Fig. 1l). All these reveal that high expression of VDR was associated with the favorable clinical outcome of GC.

Activation of VDR in GC cells inhibits CAF-induced oxaliplatin resistance

Although no positive VDR immunostaining was found in GC-CAFs, VDR's impact on tumor-stroma crosstalk was still our point of interest. To clarify this point, we firstly isolated CAFs and NFs from fresh gastric tumor and non-tumor tissues. By immunofluorescence, we identified cells with higher levels of fibroblast activation protein (FAP) and alpha-smooth muscle actin (α-SMA) than NFs as CAFs (Fig. 2a). We then set up a co-culture system that allowed GC cells to be educated with CAFs and separated for further experiments. As shown in Fig. 2b, CAFs induced stronger resistance to oxaliplatin in HGC-27 and AGS cells compared to NFs. Additionally, cancer cells co-incubated with CAFs had a decreased level of apoptosis when exposed to the drug in contrast to the control group (Fig. 2c, d). To further confirm these findings in vivo, we employed a xenograft model by injecting 1×10^7 HGC-27 cells into each mouse subcutaneously with or without 2×10^6 human CAFs ($n = 5$), and treating the mouse with oxaliplatin three times a week from the 7th day following the implantation. Results showed that in the groups xenografted with HGC-27 cells, the mean volume of the tumors in the oxaliplatin treated group was significantly smaller than that of the negative control group. However, co-injection of HGC-27 cells with CAFs dramatically sustained tumor growth in mice under oxaliplatin treatment (Fig. 2e). This highlighted that the addition of CAFs suppressed the anti-cancer effect of oxaliplatin on GC cells in vivo.

Given the association of VDR expression with CAFs oncogenic behavior in the TME [16, 17], we aimed to determine whether activation of VDR expression in GC cells affects the CAF-induced oxaliplatin resistance. Thus, we applied Cal, a synthetic VitD3 analog, with a high affinity for the Vitamin D receptor, to incubate with CAFs and GC cells, respectively. Consistent with the finding in clinical samples, VDR is negatively expressed in CAFs in vitro, and Cal significantly stimulated VDR activation in HGC27 and AGS cells, but not in CAFs' (Fig. 3a). In addition, Cal treatment suppressed the survival rate of oxaliplatin-exposed GC cells (Supplementary Fig. S1a). We harvested CAFs after incubating them with Cal, and then co-cultured it with GC cells. These Cal-treated CAFs did not showed the ability to promote chemoresistance in HGC-27 and AGS cells (Supplementary Fig. S1b). In contrast, in the other group that HGC-27 and AGS cells were pretreated with Cal and then co-cultured with CAFs, activation of VDR in GC cells significantly inhibited the tumor-supportive effect of CAFs (Fig. 3b, c). Moreover, by adding the culture medium of CAFs (CAF-CM) into the culture dish of HGC-27 and AGS cells and analyzing these GC cells with Western blot and flow analysis, we found that Cal significantly suppressed the anti-apoptotic effect of CAFs on oxaliplatin-treated HGC-27 and AGS cells (Fig. 3d, e).

To further verify the role of VDR in GC in vivo, we prepared a xenograft mouse model by inoculating HGC-27 cells mixed with CAFs in each group ($n = 7$). On the third day following the implantation, one group was injected with oxaliplatin three times a week and the other group was treated with the same dose of oxaliplatin and Cal. Sixteen days later, the group treated with both oxaliplatin and Cal formed much smaller tumors than the group treated with oxaliplatin only (Fig. 3f). Immunochemistry of harvested tumors tissues also supported that Cal induced activation of VDR and apoptosis (reflected by the downregulation of proliferation marker Ki-67) in tumors (Fig. 3g). Therefore, activation of VDR reversed the tumor-supportive effect of CAF and enhanced the anti-tumor effect of oxaliplatin by inducing apoptosis in vitro and in vivo.

Activation of VDR inhibits CAF-derived IL-8 induced chemoresistance via PI3K/AKT pathway

To uncover the mechanism underlying VDR inhibited CAF-mediated chemoresistance in GC cells, we performed transcriptome analysis on HGC-27 cells co-cultured with CAFs, with or without the presence of Cal (Fig. 4a). The RNA sequencing results showed that Cal treatment affected a wide range of genes in HGC-27 cells, with 663 and 436 genes significantly upregulated and downregulated, respectively (Fig. 4b). According to the pathway analysis, the PI3K/AKT pathway was indicated to be the most significant activated signaling pathway in HGC-27 cells following Cal treatment (Fig. 4c). The Western blot result confirmed that CAFs greatly activated PI3K/AKT signaling in HGC-27 and AGS cells. Notably, application of Cal suppressed CAF-induced PI3K/

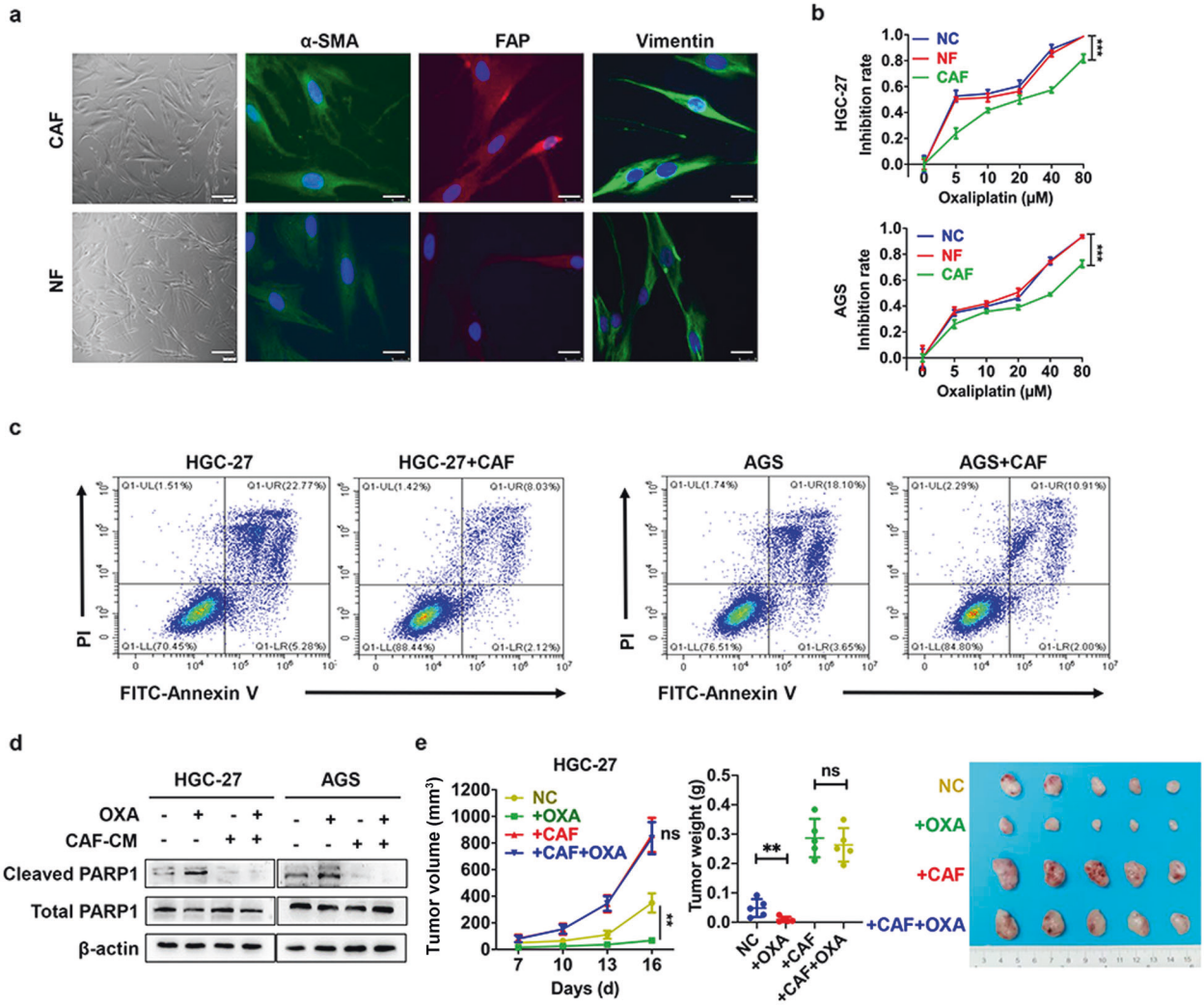

Fig. 2 Tumor-supportive effect of CAFs on GC. a Representative imaging under white light (Scale bar, 100 μm) and immunofluorescent staining (Scale bar, 25 μm) showing the expression of α-SMA, FAP and Vimentin in cancer associated fibroblasts (CAFs) and normal fibroblasts (NFs), respectively; **b** The growth inhibition rates of oxaliplatin (OXA) on HGC-27 and AGS cells pre-cultured with CAFs or NFs; **c** Flow cytometry results showed the proportion of apoptotic cells in HGC-27 and AGS cells treated with OXA (10 μM) for 24 h, pre-cultured with or without CAFs; **d** Immunoblot for cleaved/total PARP in OXA-treated HGC-27 and AGS cells pre-cultured with or without CAFs; **e** Tumor growth (left) and weight (middle) curves and tumor images (right) at day 16th. **f** Representative images showing H&E staining and IHC staining for Ki-67 in harvested xenograft tumors. $^{*}P < 0.05$, $^{**}P < 0.01$, $^{***}P < 0.001$

AKT pathway activation in cancer cells **(**Fig. 4d**)**. Furthermore, inhibition of VDR with siRNA partly reversed the activation effect of Cal on the PI3K/AKT pathway **(**Supplementary Fig. S2). To verify the critical role of the PI3K/AKT pathway in the tumor-supportive effect of CAFs, HGC-27 and AGS cells were incubated with two different kinds of PI3K/AKT pathway inhibitors, perifosine and 3-methyladenine, for 24 h and then co-cultured with CAFs. Results indicated that CAFs-mediated chemoresistance was largely attenuated by blocking PI3K/AKT pathway **(**Fig. 4e**)**. In addition, by in vivo experiment, we also confirmed that inhibition of the PI3K/AKT pathway significantly blocked CAF-induced chemoresistance, and 3-methyladenine treatment suppressed the activation of PI3K/AKT pathway and Ki-67 expression (Supplementary Fig. S3). Furthermore, we detected the immunostaining of P-AKT in tumor tissues harvested from a xenograft mouse model in Fig. 3f, the result also revealed that Cal downregulated PI3K/AKT pathway in vivo (Supplementary Fig. S4). Thus, VDR activation abrogates CAF-induced oxaliplatin resistance by inhibiting PI3K/AKT pathway in GC cells.

Cytokine and chemokines are the indispensable media in crosstalk between cancer cells and the TME. To explore how CAFs induce PI3K/AKT pathway activation in GC, we applied RayBio Human Cytokine Antibody Array to detect the cytokines in the conditioned medium (CM) of CAFs and HGC-27 cells (Fig. 4f). IL-8 showed the most significant up-regulation among the ten most differentially secreted cytokines between CAF and HGC-27 cells (fold change 4.73; Fig. 4g). ELISA assay further confirmed that CAFs secreted a higher level of IL-8 than HGC-27 and AGS cells (Fig. 4h). The relationship between CAFs and IL-8 was further confirmed by double immunofluorescence analyses of FAP and IL-8 in tumor tissue samples of patients with GC. As shown in Fig. 4i, IL-8 was mainly expressed in GC cells and CAFs. In addition, the level of IL-8 was significantly associated with the CAF marker FAP expression in GC tissues of 407 patients in the TCGA database **(**Supplementary Fig. S5).

We then detected whether CAFs-derived IL-8 activated the PI3K/AKT pathway in GC cells. As shown in Fig. 4j, IL-8 receptor CXCR2 was up-regulated in CAFs-CM incubated HGC-27 and AGS

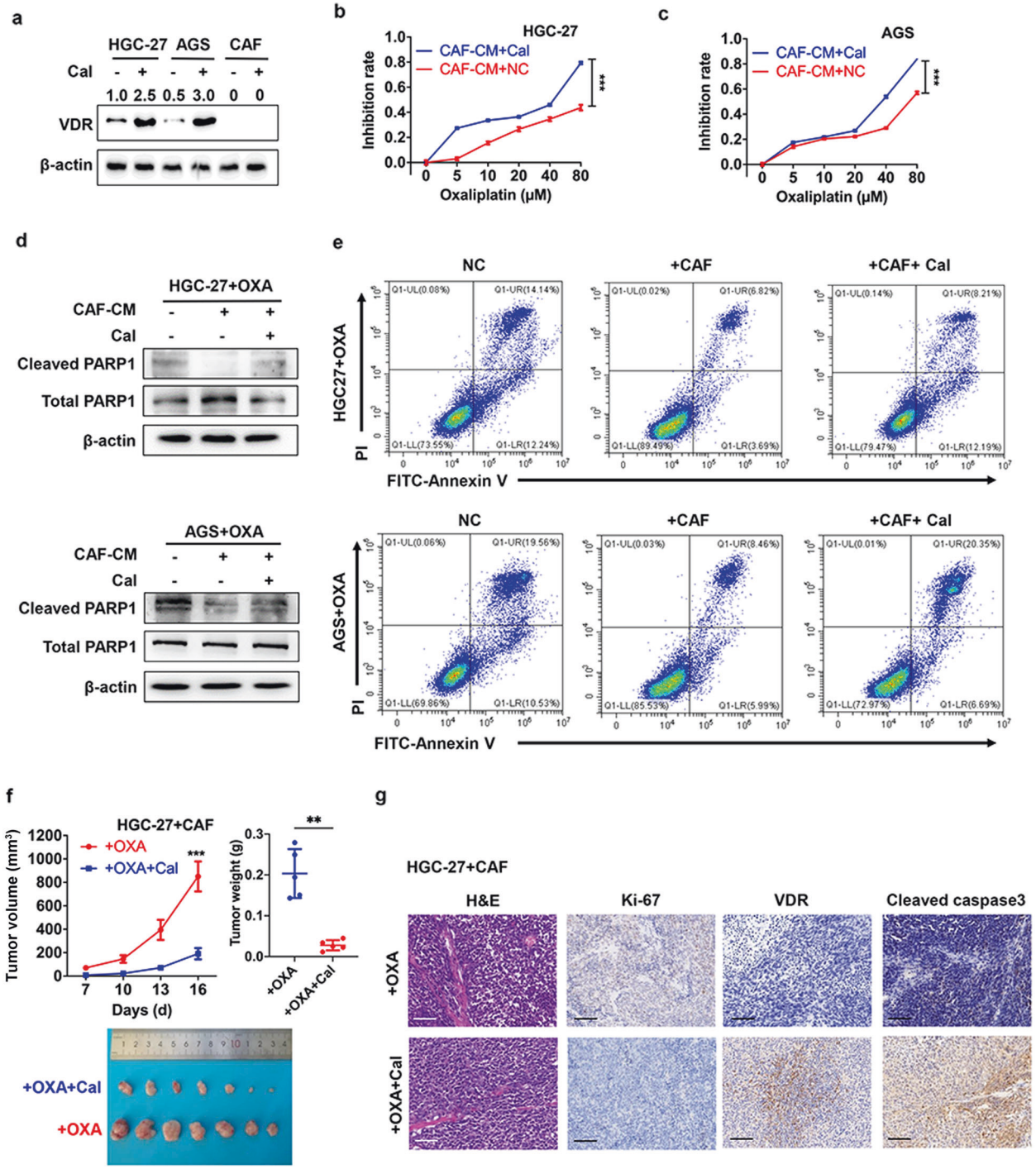

Fig. 3 Activation of VDR in GC cells reverses CAF-mediated chemoresistance. a Immunoblot for VDR expression in CAFs, HGC-27 and AGS cells under Cal (500 μM) treatment for 24 h; **b**, **c** The growth inhibition rates of OXA on CAFs co-cultured GC cells under treatment with or without Cal (500 nM) for 24 h; **d** Immunoblot for total and cleaved PARP1 in HGC-27 and AGS cells treated for 24 h with OXA, OXA + CAF-CM, or OXA + CAF-CM + Cal, respectively; **e** Flow cytometry results showed the proportion of apoptotic cells in HGC-27 and AGS cells treated for 24 h with OXA, OXA + CAF-CM, or OXA + CAF-CM + Cal; **f** Tumor growth (left) and weight (right) curves and tumor images (bottom) at day 16; **g** Representative images showing H&E staining and IHC staining for Ki-67, VDR and cleaved caspase-3 in xenograft tumors harvested from the indicated groups. Scale bar = 100 μm; $^{**}P < 0.01$, $^{***}P < 0.001$

cells, followed by activation of PI3K/AKT pathway. Similar results were also found in HGC-27 and AGS cells with IL-8 treatment. However, the addition of IL-8 neutralizing antibody (anti-IL-8) in CAFs-CM drastically attenuated the pro-tumoral effect of CAFs. Moreover, knockdown of CXCR2 also effectively hesitated IL-8-induced activation of the PI3K/AKT pathway (Supplementary Fig. S6). Thus, secretion of IL-8 from CAFs stimulated PI3K/AKT pathway by targeting CXCR2 in gastric cells. In addition, CAFs derived IL-8 is the main cause for tumor chemoresistance, whereas neutralized IL-8 in the CAF-CM can abolish CAF-mediated oxaliplatin resistance. The addition of IL-8 alone could contribute to GC drug resistance. However, activation of VDR by Cal-

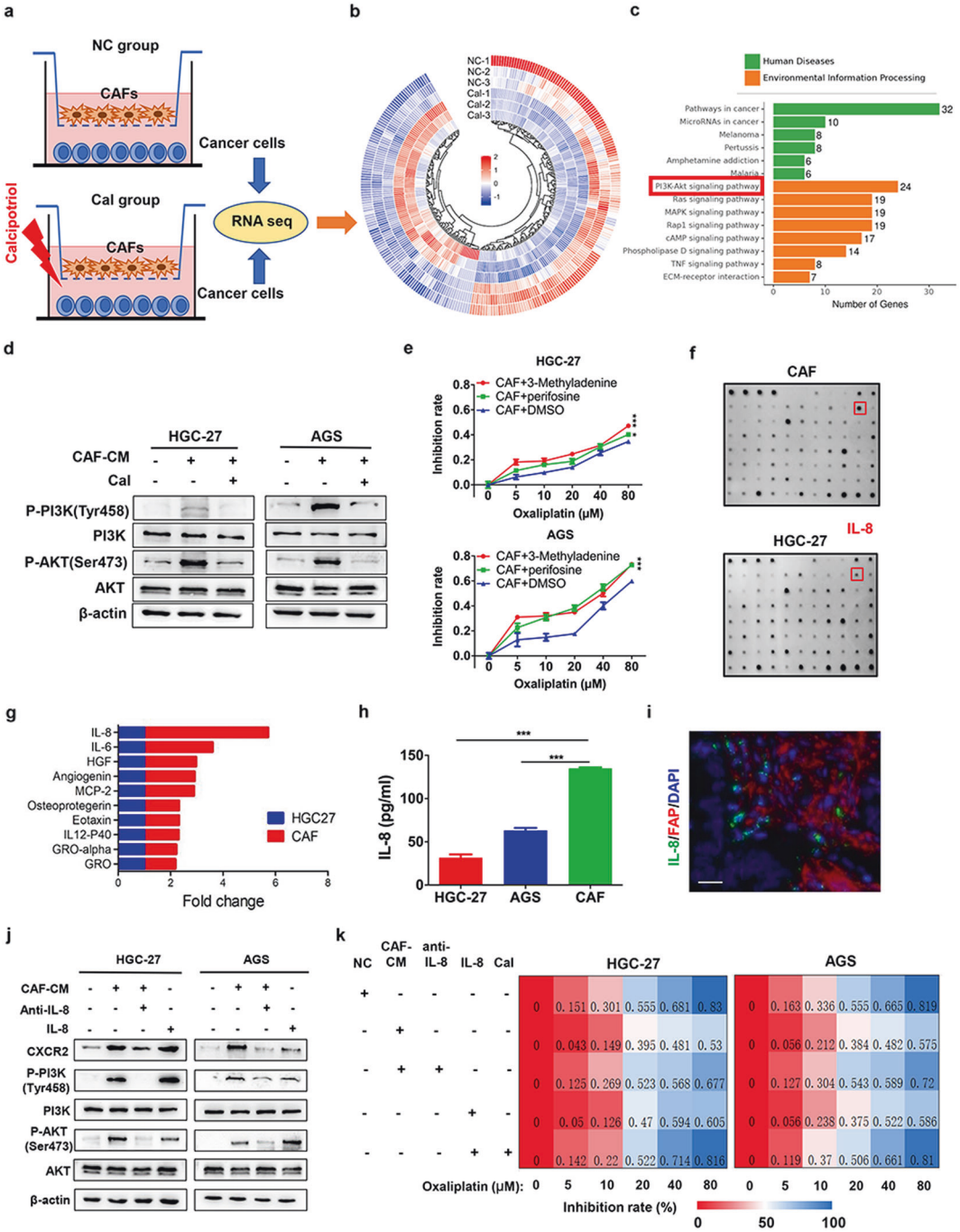

Fig. 4 Cal inhibits oxaliplatin (OXA) resistance induced by CAF by blocking IL-8/PI3K/AKT pathway. a Protocol of preparing cell samples for RNA sequencing. HGC-27 cells were incubated with CAFs in the presence or absence of Cal for 48 h; **b** Heatmap representing significantly dysregulated genes from RNA-seq analysis ($n = 3$); **c** Pathway analysis of differentially expressed genes in HGC-27 cells co-cultured with CAFs treated with or without Cal; **d** Immunoblot for expression of P-PI3K, PI3K, P-AKT, AKT in CAF-treated HGC-27 cells in the presence or absence of Cal for 48 h; **e** The growth inhibition rates of OXA on HGC-27 or AGS cells co-cultured with CAFs, under treatment with two different kinds of PI3K/AKT inhibitors, 3-methyladenine (5 mM) and perifosine (10 μM) for 48 h (***$P < 0.001$); **f** The profiles of cytokines produced by CAFs and HGC-27 cells examined by RayBio Human Cytokine Antibody Array, red arrow represents the most significantly overexpressed cytokine IL-8; **g** The top ten cytokines most differentially expressed in supernatant of CAFs and HGC-27 cells, detected by RayBio Human Cytokine Antibody Array; **h** Elisa assay was performed to detect the amount of soluble IL-8 in supernatant of CAFs, HGC-27 and AGS cells; **i** Representative image of double immunofluorescence showing IL-8 and CAF marker FAP expression in tissues of GC (scale bar, 20 μm); **j** Immunoblot for CXCR2, P-PI3K, PI3K, P-AKT, AKT expression in HGC-27 and AGS cells treated with CAF-CM, CAF-CM + anti-IL-8 (IL-8 neutralizing antibody, 1 μg/mL), or IL-8 (200 ng/mL) alone for 24 h; **k** The growth inhibition rates of oxaliplatin (OXA) on HGC-27 and AGS cells treated with CAF-CM, CAF-CM + anti-IL-8 (IL-8 neutralizing antibody, 1 μg/mL), IL-8 (200 ng/mL), or Cal (500 nM) for 24 h. ***$P < 0.001$

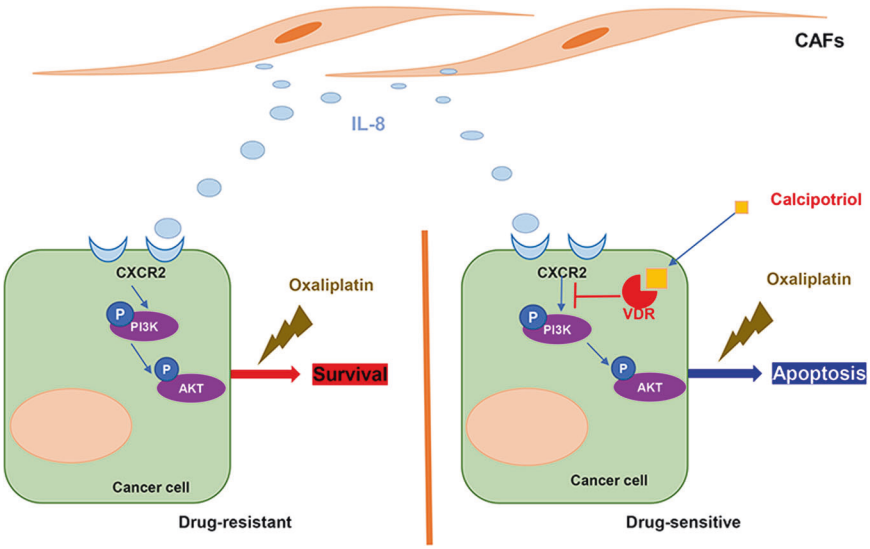

Fig. 5 A schematic diagram illustrates the effect of VDR activation on CAF-mediated chemoresistance in GC. CAFs can induce oxaliplatin resistance in GC cells by activating PI3K/AKT via IL-8 secretion. Activation of VDR by VitD3 analogue Cal can abolish CAF-induced drug resistance and induce apoptosis through targeting PI3K/AKT pathway in cancer cells. IL-8, interleukin 8; CAFs, cancer-associated fibroblasts; VDR, Vitamin D receptor

treatment largely abrogated the tumor-supportive effect of IL-8 on carcinoma cells **(**Fig. 4k**)**. In summary, activation of VDR abrogated CAFs-derived IL-8-mediated chemoresistance via blocking PI3K/Akt signaling pathway in GC. A schema illustrated the role and mechanism underlying the effects of VDR in hesitating CAF-mediated chemoresistance in GC (Fig. 5).

DISCUSSION

The basic structure of tumor micro-organs is composed of cancer cells, endothelial cells, pericytes, fibroblasts, various white blood cells, and extracellular matrix. In the process of malignant progression, the surrounding TME co-evolves into an active state through paracrine, juxtracrine, and autocrine communication, thereby creating a dynamic signal that contributes to the occurrence and development of cancer, as well as drug resistance [7]. The importance of TME has been confirmed by a number of studies, which demonstrated the correlation between the gene expression patterns in microenvironmental cells and prognoses of patients with pancreatic cancer [23], colorectal cancer [24] and GC [25]. Thus, as a target for cancer treatment and a rich source of biomarkers with prognostic and/or predictive potential, TME is attracting people's attention. By identifying tumor-related regulatory molecules, exploring their significance in the dialogue between TME and tumor cells, as well as their molecular biological mechanisms, this study will undoubtedly shed new light on elucidating tumor development mechanisms and targeted therapy.

Recently, cumulative clinical and fundamental studies have shown that Vitamin D ameliorates the incidence and mortality of many cancers [13, 14, 17, 26]. Indeed, the biological actions of 1,25 $(OH)_2D_3$ are mainly mediated by Vitamin D receptors (VDR). VDR has been implicated in the regulation of malignancies through the TME approach in many ways. For example, VDR exerts an antiproliferative effect in endothelial cell [27]; enhances NK cells-induced cytotoxicity and downregulates breast cancer cell viability [28]. In pancreatic cancer, VDR enhances chemotherapeutic response through reprising the quiescent state of pancreatic stellate cells and increasing intra-tumoral gemcitabine [16]; activation of VDR can also limit the tumoral-supportive effects of CAFs via inhibiting exosomal miR-10a-5p transmission from CAFs to pancreatic cancer cells [29]. Several studies have detailed the effects of Vitamin D on GC cells [30, 31], and a previous study that analyzed VDR immunostaining in tumor samples from a set of 92 patients with GC has reported that VDR expression was significantly lower in GC tissues, and highly expressed in well and moderate differentiated GC tissues, as well as in GC tissues with small size [18]. Although we found no significant difference in VDR protein expression between GC samples and normal gastric mucus, our current results also confirmed that VDR has lower expression in GC samples with more malignant clinical phenotype and advanced clinical stages. VDR has been reported widely expressed in stroma from human pancreatic and colorectal tumors [16, 17, 29]. However, few studies have illustrated the potential profile and role of VDR considering the presence of the tumor microenvironment in GC. Our study highlighted that high expression of VDR in tumor tissue was associated with longer overall survival (OS) in GC patients. However, no positive immunostaining of VDR was found in GC-CAFs. Activation of VDR by VD analog Cal reversed CAF-induced chemoresistance in vitro and in vivo by targeting GC cells, not stromal fibroblasts. This result widens our knowledge of the distribution of VDR in the TME of GC and indicates that VDR may exerts its anti-tumoral action by directly affecting gastric carcinoma cells.

Various reports showed that the active form of Vitamin D, 1α,25-dihydroxy Vitamin D3 (1,25$(OH)_2D_3$) suppressed GC cell growth by targeting antiproliferative miRNAs [31, 32] or oncogenic signaling [30, 33]. Interestingly, there have been various evidences showing that VDR expression is specifically expressed in the CAFs of TME [16, 17], and high VDR expression in CAFs is associated with longer survival of patients with cancer [17]. Accordingly, VDR can impede TGF-β/SMADs signaling in myofibroblasts [34]; activation of VDR within fibroblasts reduces CXCL12 secretion and thus suppresses the pro-tumorigenic crosstalk between CAF and cancer cells [35]. These data have innovatively proposed the mechanism by which VDR participates in the malignant biological behavior of tumor cells via regulating tumor stromal cells. However, it also raised the question that whether VDR, which was specifically expressed in GC cells, can also functionally participated in the crosstalk between CAFs and GC cells. The present study was focused on this topic and verified that 1,25$(OH)_2D_3$ has additional anti-cancer effects in GC cells by targeting the intracellular pro-tumoral signaling which

was activated by stromal fibroblasts derived cytokines. Thus, the therapeutic effect of VDR agonists is not only to modulate tumor cells biology, but also to affect the crosstalk between CAFs and tumor cells. Our data support the possible beneficial effects of therapies using VDR agonists against GC.

CAFs in the tumor microenvironment contribute much to cancer cells in different situations. Cytokines and chemokines are the critical media in crosstalk between cancer cells and stromal cells. They are soluble secreted proteins produced by complex components in the tumor microenvironment and exert tremendous effects on target cells. IL-8, as commonly identified cytokines secreted by cancer-derived stromal cells [36], has been widely implicated in the malignant behaviors of cancer cells and serves as a tumor-supportive factor [10, 37, 38]. Here, we applied a human cytokine antibody array to find out that CAFs secrete IL-8 to induce oxaliplatin resistance in GC cells, while activation of VDR by Cal largely abrogated its pro-tumoral effect in GC cells. In addition, the application of RNA sequencing indicated that Cal activated VDR to inhibit the pro-tumoral effect of stroma via PI3K/AKT pathway. Our findings reinforce the relevance of tumor stroma and tumor microenvironment as targets for anticancer therapies and strongly support $1,25(OH)_2D_3$ as an important and multifaceted protective agent in GC. Whether the suppressive effect of $1,25(OH)_2D_3$ on IL-8, as well as its downstream PI3K/AKT pathway, is universal in human malignancies requires extensive analysis.

CAFs are quite universal but not the most abundant cellular component of TME. Although we also observed the expression of VDR in GC-associated lymphocytes, no significant association between VDR expression in this cell type and clinical outcome has been found in our cohort (data not shown). The result from our RNA-seq analysis indicate that several chemokines and extracellular matrix proteins with immune cell chemoattractant potential were $1,25(OH)_2D_3$ target genes in CAFs. Thus, $1,25(OH)_2D_3$ may indirectly modulate tumor-stromal lymphocyte properties through its action on cancer cells. In addition, the expression and putative role of VDR in gastric tumor-stromal endothelial cells and immune cell types other than lymphocytes remain unexplored.

In conclusion, we demonstrated that VDR activation could strongly abolish the drug resistance of GC cells mediated by CAFs under oxaliplatin treatment. Vitamin D might be a protective agent in GC chemotherapy.

DATA AVAILABILITY

All data generated and described in this article are available from the corresponding author on reasonable request.

ACKNOWLEDGEMENTS

This work was supported by National Natural Science Foundation of China (81972249, 82172702, 81902430), Shanghai Clinical Science and Technology Innovation Project of Municipal Hospital (SHDC12020102), Clinical Research Project of Shanghai Shenkang Hospital Development Center (SHDC2020CR4068), Natural Science Foundation of Shanghai (21ZR1414900, 22ZR1413000), Artificial Intelligence Medical Hospital Cooperation Project of Xuhui District (2021-017), Shanghai Science and Technology Development Fund (19MC1911000), Shanghai Municipal Key Clinical Specialty (shslczdzk01301), Shanghai "Rising Stars of Medical Talents" Youth Development Program Youth Medical Talents – Specialist Program (SHWSRS(2020)_087).

AUTHOR CONTRIBUTIONS

MDX, ZXZ, YQZ and HS conceived the study, performed the literature search and bioinformatics analysis, and prepared the figures. ZQC, JJC, XinW, CT, ZQC, SJN, WWW, MZ, DH, LW and XuW helped with data collection, analysis, and interpretation. YF, MDX and WQS wrote and revised the manuscript. All authors read and approved the final manuscript.

ADDITIONAL INFORMATION

Supplementary information The online version contains supplementary material available at https://doi.org/10.1038/s41401-022-00927-1.

Competing interests: The authors declare no competing interests.

REFERENCES

1. Sung H, Ferlay J, Siegel RL, Laversanne M, Soerjomataram I, Jemal A, et al. Global Cancer Statistics 2020: GLOBOCAN estimates of incidence and mortality worldwide for 36 cancers in 185 countries. CA Cancer J Clin. 2021;71:209–49.
2. Smyth EC, Nilsson M, Grabsch HI, van Grieken NCT, Lordick F. Gastric cancer. Lancet. 2020;396:635–48.
3. Ajani JA, D'Amico TA, Bentrem DJ, Chao J, Cooke D, Corvera C, et al. Gastric Cancer, Version 2.2022, NCCN Clinical Practice Guidelines in Oncology. J Natl Compr Canc Netw. 2022;20:167–92.
4. Biagioni A, Skalamera I, Peri S, Schiavone N, Cianchi F, Giommoni E, et al. Update on gastric cancer treatments and gene therapies. Cancer Metastasis Rev. 2019;38:537–48.
5. Hanahan D, Coussens LM. Accessories to the crime: functions of cells recruited to the tumor microenvironment. Cancer Cell. 2012;21:309–22.
6. Park D, Sahai E, Rullan A. SnapShot: cancer-associated fibroblasts. Cell. 2020;181:486.
7. Chen X, Song E. Turning foes to friends: targeting cancer-associated fibroblasts. Nat Rev Drug Discov. 2019;18:99–115.
8. Kobayashi H, Enomoto A, Woods SL, Burt AD, Takahashi M, Worthley DL. Cancer-associated fibroblasts in gastrointestinal cancer. Nat Rev Gastroenterol Hepatol. 2019;16:282–95.
9. Oya Y, Hayakawa Y, Koike K. Tumor microenvironment in gastric cancers. Cancer Sci. 2020;111:2696–707.
10. Zhai J, Shen J, Xie G, Wu J, He M, Gao L, et al. Cancer-associated fibroblasts-derived IL-8 mediates resistance to cisplatin in human gastric cancer. Cancer Lett. 2019;454:37–43.
11. Ji Z, Tian W, Gao W, Zang R, Wang H, Yang G. Cancer-associated fibroblast-derived interleukin-8 promotes ovarian cancer cell stemness and malignancy through the notch3-mediated signaling. Front Cell Dev Biol. 2021;9:684505.
12. Chen C, Zhang R, Ma L, Li Q, Zhao YL, Zhang GJ, et al. Neuropilin-1 is up-regulated by cancer-associated fibroblast-secreted IL-8 and associated with cell proliferation of gallbladder cancer. J Cell Mol Med. 2020;24:12608–18.
13. Morita M, Okuyama M, Akutsu T, Ohdaira H, Suzuki Y, Urashima M. Vitamin D supplementation regulates postoperative serum levels of PD-L1 in patients with digestive tract cancer and improves survivals in the highest quintile of PD-L1: a post Hoc analysis of the AMATERASU randomized controlled trial. Nutrients. 2021;13:1987.
14. Chandler PD, Chen WY, Ajala ON, Hazra A, Cook N, Bubes V, et al. Effect of vitamin D3 supplements on development of advanced cancer: a secondary analysis of the VITAL randomized clinical trial. JAMA Netw Open. 2020;3:e2025850.
15. Yuan C, Ng K. Vitamin D supplementation: a potential therapeutic agent for metastatic colorectal cancer. Br J Cancer. 2020;123:1205–6.
16. Sherman MH, Yu RT, Engle DD, Ding N, Atkins AR, Tiriac H, et al. Vitamin D receptor-mediated stromal reprogramming suppresses pancreatitis and enhances pancreatic cancer therapy. Cell. 2014;159:80–93.
17. Ferrer-Mayorga G, Gomez-Lopez G, Barbachano A, Fernandez-Barral A, Pena C, Pisano DG, et al. Vitamin D receptor expression and associated gene signature in tumour stromal fibroblasts predict clinical outcome in colorectal cancer. Gut. 2017;66:1449–62.
18. Wen Y, Da M, Zhang Y, Peng L, Yao J, Duan Y. Alterations in vitamin D signaling pathway in gastric cancer progression: a study of vitamin D receptor expression in human normal, premalignant, and malignant gastric tissue. Int J Clin Exp Pathol. 2015;8:13176–84.
19. Chen LW, Chang LC, Hua CC, Cheng TC, Lee CC. Comparing the expressions of Vitamin D receptor, cell proliferation, and apoptosis in gastric mucosa with gastritis, intestinal metaplasia, or adenocarcinoma change. Front Med (Lausanne). 2021;8:766061.
20. Sun H, Chang J, Ye M, Weng W, Zhang M, Ni S, et al. GCNT4 is associated with prognosis and suppress cell proliferation in gastric cancer. OncoTargets Ther. 2020;13:8601–13.
21. Sun H, Ni SJ, Ye M, Weng W, Zhang Q, Zhang M, et al. Hedgehog interacting protein 1 is a prognostic marker and suppresses cell metastasis in gastric cancer. J Cancer. 2018;9:4642–9.
22. Dottermusch M, Krüger S, Behrens HM, Halske C, Röcken C. Expression of the potential therapeutic target claudin-18.2 is frequently decreased in gastric cancer: results from a large Caucasian cohort study. Virchows Arch. 2019;475:563–71.
23. Francescone R, Barbosa Vendramini-Costa D, Franco-Barraza J, Wagner J, Muir A, Lau AN, et al. Netrin G1 promotes pancreatic tumorigenesis through cancer-

associated fibroblast-driven nutritional support and immunosuppression. Cancer Discov. 2021;11:446–79.
24. Heichler C, Scheibe K, Schmied A, Geppert CI, Schmid B, Wirtz S, et al. STAT3 activation through IL-6/IL-11 in cancer-associated fibroblasts promotes colorectal tumour development and correlates with poor prognosis. Gut. 2020;69:1269–82.
25. Jin Z, Lu Y, Wu X, Pan T, Yu Z, Hou J, et al. The cross-talk between tumor cells and activated fibroblasts mediated by lactate/BDNF/TrkB signaling promotes acquired resistance to anlotinib in human gastric cancer. Redox Biol. 2021;46:102076.
26. Johansson H, Spadola G, Tosti G, Mandala M, Minisini AM, Queirolo P, et al. Vitamin D supplementation and disease-free survival in stage II melanoma: a randomized placebo controlled trial. Nutrients. 2021;13:1931.
27. Chung I, Wong MK, Flynn G, Yu WD, Johnson CS, Trump DL. Differential anti-proliferative effects of calcitriol on tumor-derived and matrigel-derived endothelial cells. Cancer Res. 2006;66:8565–73.
28. Min D, Lv XB, Wang X, Zhang B, Meng W, Yu F, et al. Downregulation of miR-302c and miR-520c by $1,25(OH)_2D_3$ treatment enhances the susceptibility of tumour cells to natural killer cell-mediated cytotoxicity. Br J Cancer. 2013;109:723–30.
29. Kong F, Li L, Wang G, Deng X, Li Z, Kong X. VDR signaling inhibits cancer-associated-fibroblasts' release of exosomal miR-10a-5p and limits their supportive effects on pancreatic cancer cells. Gut. 2019;68:950–1.
30. Li Q, Li Y, Jiang H, Xiao Z, Wu X, Zhang H, et al. Vitamin D suppressed gastric cancer cell growth through downregulating CD44 expression in vitro and in vivo. Nutrition. 2021;91-92:111413.
31. Chang S, Gao Z, Yang Y, He K, Wang X, Wang L, et al. miR-99b-3p is induced by vitamin D3 and contributes to its antiproliferative effects in gastric cancer cells by targeting HoxD3. Biol Chem. 2019; 400:1079–86
32. Chang S, Gao L, Yang Y, Tong D, Guo B, Liu L, et al. miR-145 mediates the antiproliferative and gene regulatory effects of vitamin D3 by directly targeting E2F3 in gastric cancer cells. Oncotarget. 2015;6:7675–85.
33. Bao A, Li Y, Tong Y, Zheng H, Wu W, Wei C. Tumor-suppressive effects of 1, 25-dihydroxyvitamin D3 in gastric cancer cells. Hepatogastroenterology. 2013;60:943–8.
34. Shany S, Sigal-Batikoff I, Lamprecht S. Vitamin D and myofibroblasts in fibrosis and cancer: at cross-purposes with TGF-beta/SMAD signaling. Anticancer Res. 2016;36:6225–34.
35. Anbil S, Pigula M, Huang HC, Mallidi S, Broekgaarden M, Baglo Y, et al. Vitamin D receptor activation and photodynamic priming enables durable low-dose chemotherapy. Mol Cancer Ther. 2020;19:1308–19.
36. Bussard KM, Mutkus L, Stumpf K, Gomez-Manzano C, Marini FC. Tumor-associated stromal cells as key contributors to the tumor microenvironment. Breast Cancer Res. 2016;18:84.
37. Bae WJ, Ahn JM, Byeon HE, Kim S, Lee D. PTPRD-inactivation-induced CXCL8 promotes angiogenesis and metastasis in gastric cancer and is inhibited by metformin. J Exp Clin Cancer Res. 2019;38:484.
38. Fang T, Lv H, Lv G, Li T, Wang C, Han Q, et al. Tumor-derived exosomal miR-1247-3p induces cancer-associated fibroblast activation to foster lung metastasis of liver cancer. Nat Commun. 2018;9:191.